

Tall clouds from small eruptions: the sensitivity of eruption height and fine ash content to tropospheric instability

Andrew Tupper · Christiane Textor · Michael Herzog ·
Hans-F. Graf · Michael S. Richards

Received: 9 February 2008 / Accepted: 20 July 2009 / Published online: 2 September 2009
© Springer Science+Business Media B.V. 2009

Abstract A critical factor in successfully monitoring and forecasting volcanic ash dispersion for aviation safety is the height reached by eruption clouds, which is affected by environmental factors, such as wind shear and atmospheric instability. Following earlier work using the Active Tracer High Resolution Atmospheric Model for strong Plinian eruptions, this study considered a range of eruption strengths in different atmospheres. The results suggest that relatively weak volcanic eruptions in the moist tropics can trigger deep convection that transports volcanic material to 15–20 km. For the same volcanic strength there can be ~9 km difference between eruption heights in moist tropical and dry sub-polar environments (a larger height difference than previously suggested), which appears consistent with observations. These results suggest that eruption intensity should not be estimated from eruption height alone for tropospheric eruptions and also that the average height of volcanic eruptions may increase if the tropical atmospheric belt widens in a changing climate. Ash aggregation is promoted by hydrometeors (particularly liquid

A. Tupper (✉)

Northern Territory Regional Office, Bureau of Meteorology, PO Box 40050,
Casuarina, NT 0811, Australia
e-mail: A.Tupper@bom.gov.au

A. Tupper

School of Mathematical Sciences, Monash University, Clayton, Vic, Australia

C. Textor

Deutsche IPCC-Koordinierungsstelle Projektträger im DLR Umwelt, Kultur, Nachhaltigkeit Heinrich-Konen-Str.153227, Bonn, Germany

M. Herzog · H.-F. Graf

Centre Atmospheric Sciences, University of Cambridge, Cambridge, UK

M. S. Richards

Cooperative Institute for Meteorological Satellite Studies, University of Wisconsin,
Madison, WI, USA

Present Address:

M. S. Richards

Federal Aviation Administration, Atlantic City, OK, USA

water), so the smaller modelled eruptions in moist atmospheres, which have a relatively small ash content for their height and water content, result in a relatively small proportion of fine ash in the dispersing cloud when compared to a dry atmosphere. This in turn makes the ash clouds much more difficult to detect using remote sensing than those in dry atmospheres. Overall, a weak eruption in the tropics is more likely to produce a plume above cruising levels for civil aviation, harder to detect and track, but with a lower concentration of fine ash than a mid-latitude or polar equivalent. There is currently no defined ‘acceptable’ concentration of ash for aircraft, but as these results suggest low-grade encounters in the tropics from undetected clouds are likely, it would be desirable to explore that issue.

Keywords Volcanic eruption column modelling · Aviation safety · Volcanic eruptions · Remote sensing · Volcanic climate effects · Volcanic dynamics

1 Introduction

1.1 The importance of eruption height

During a volcanic eruption, the height reached by a volcanic eruption column is important for evaluation of where ashfall may occur, for an understanding of the extent of stratospheric injection (e.g. Halmer and Schmincke 2003), and, therefore, whether there may be significant climate effects (Robock 2002). Another reason for knowing the cloud height, and the focus of this paper, is to forecast the area that aircraft should avoid flying in as the ash cloud disperses (International Civil Aviation Organization 2009). Two quantities are particularly significant: the approximate maximum cloud height to define the layers of atmosphere where the risk exists, and the height(s) of maximum ash dispersion (the neutral buoyancy height in the case of a single umbrella cloud), to determine where the most significant drifting ash clouds should be. These values are often problematic to observe directly (Tupper et al. 2007), and so it is extremely useful to have a refined understanding of how plumes (used here in the sense of ‘clouds’ still attached to the source volcano) might or should develop given a particular kind of eruption into a particular atmosphere, and use that to initialise atmospheric dispersion models and to aid satellite analysis.

1.2 Volcanic cloud height dependency on atmospheric water content, temperature, tropopause height and wind shear

A number of important studies, briefly summarised here, have given us an insight into the kind of height variations to expect between different atmospheric environments.

Sparks et al. (1997) and Woods (1988, 1998) summarise much of the observational and modelling work done on eruption columns. Early work on plume heights was done by Morton et al. (1956), who used scaling arguments to show that the height of volcanic plumes should be related to the fourth root of the eruptive power (roughly the fourth root of mass eruption rate). Wilson et al. (1978) examined and further developed models of maintained and noncontinuous plumes. For maintained plumes, they compared theoretical predictions to some presatellite era observations of volcanic plume heights, and found rough agreement. Their results for noncontinuous plumes were inconclusive.

Settle (1978) similarly compared cloud height observations with results of scaling arguments to find rough agreement, although noting issues with the height observations

used (discussed further below). Observations used by these and other authors were later combined to produce an empirical best-fit curve giving an approximate cloud height for a given dense rock equivalent discharge rate of magma (Sparks et al. 1997, eq. 5.1).

Using 1-D ‘top hat’ modelling and the US Standard Atmosphere, Woods (1993, 1998) suggested that for large eruptions, the largest component of the water budget originates from magmatic water, but that for small eruption columns, ascending to 8–10 km, the entrained water vapour constitutes a much larger mass than the original magmatic water. The moisture profile within the troposphere therefore determines how much moisture is entrained as the cloud ascends, and how much latent heat can be released during column ascent. Woods modelled a modest (2–3 km) increase in eruption height for smaller eruptions due to latent heat release from this entrained water vapour, and also suggested that there might be an analogy between this effect and convective plumes above fields of burning sugar cane.

Glaze and Baloga (1996) modelled the neutral buoyancy height for a range of temperature profiles, suggesting a large height variation for small steam plumes (between several tens to hundreds of metres high), but a milder variation with temperature gradient and with tropopause height for larger volcanic plume height. Woods (1995) shows the importance of the tropopause for large eruptions since polar tropopauses can be at around 8 km, and tropical tropopauses at 17 km or more.

Glaze et al. (1997) extended their previous work to consider the transport of water into the stratosphere, using a model similar to Woods (1993) but with some refinements, particularly to the treatment of condensation during column rise. They confirmed the result of Woods (1993) that for eruption rates greater than $\sim 10^7 \text{ kg s}^{-1}$, magmatic water dominates entrained water in the eruption column. They also showed a height difference of around 4 km for an eruption of this strength erupted into ‘wet’ and ‘dry’ atmospheres. For their ‘wet’ and ‘dry’ atmospheres, they used latitudinally averaged observation profiles from 10°N in July 1984 (summer) and 60°N in January 1984 (winter), respectively. In this paper, we use ‘wet’ and ‘dry’ in a similar general sense, to mean moist, convectively unstable near-equatorial soundings as opposed to dry, more stable mid-latitude or polar soundings.

The wind profile of the atmosphere has a significant influence on the height that the plume can ascend to, particularly for smaller eruptions, but also for large eruptions that may interact with the polar (or presumably subtropical) jet stream (Bursik 2001). Wind also determines what direction(s) plumes will disperse, affects the entrainment rate, and also produces structural effects in the plume, such as plume ‘bifurcation’ (Ernst et al. 1994).

Graf et al. (1999) used the ‘ATHAM’ model (introduced below) in 2D Cartesian and cylindrical form to investigate (1) wind and (2) temperature gradient, humidity and tropopause effects, respectively for a simulated Plinian eruption.

1.3 Observations of volcanic plumes

Many of the plume heights used in observational examinations have been presatellite era, and have therefore relied on close measurements from the ground or even inferred from tephra dispersal (thus indicating the likely height of the umbrella cloud rather than the maximum column height). Not all observations used are considered reliable; for example Settle (1978) notes ‘... the height of an eruption cloud is typically reported to the nearest kilometre without specific reference to sea level or the elevation of the observer, and with no explicit assessment of the accuracy of the measurement...’. Sparks et al. (1997) comment that the observational data on volcanic plumes are ‘surprisingly meagre’ and repeat the concerns of Settle (1978).

In recent years, the introduction of geostationary satellites has allowed many more detailed studies, albeit still with an hourly time interval between images in many cases, and a coarser spatial resolution ($\sim 1\text{--}5$ km) than many polar-orbiting satellites. Oppenheimer (1998) reviews satellite height estimation techniques, and studies such as by Sawada (1987) and Holasek et al. (1996) show the detailed information that can be extracted from satellite data. The creation of the International Airways Volcano Watch (e.g. Tupper et al. 2007) has resulted in a stream of real-time and postanalysed cloud heights.

Although the use of these observations has still been limited by the lack of detailed information about conditions at the eruption source, some interesting results have been observed. An approximate grouping of ground-based eruption heights with latitude was done by Sawada (2002), based mostly on his 1980s work. Sawada drew few definite conclusions, but of significance was his comparison between ground-based and satellite-based eruption observations, which seemed to show a strong tendency for satellite-based eruption heights to cluster near the tropopause, and a relative lack of eruption heights in the mid-upper troposphere. The correlation between ground and satellite-based observations was also very poor.

Some of Sawada's data was used with further analyses to focus on the Asia/Pacific tropics (Tupper and Wunderman 2009), where again a poor correlation between ground-based and satellite-based observations was found (with strong underestimation of cloud heights from the ground), and a definite clustering of cloud heights near the tropopause. Many of these eruption clouds have appeared ice and gas-rich, apparently not just from ground or sea water entering the vent (e.g. Rose et al. 1995) but from entrained or magmatic water. This in turn has posed remote sensing problems when trying to identify possible ash in clouds for real-time warnings, and has been a hot topic in remote sensing circles (Prata 1989; Prata et al. 2001; Rose et al. 1995; Simpson et al. 2000, 2001; Tupper et al. 2004, 2007).

1.4 PyroCb and volcanicCb

Further to the analogy of Woods (1993) between convective enhancement of smaller volcanic clouds and pyrocumulus, there has been considerable progress in recent years in understanding pyrocumulonimbus (pyroCb, highly convective volcanic clouds triggered by fire) and the volcanic equivalent (volcanicCb). In the case of pyroCb, large stratospheric injection events have been observed to develop in unstable or conditionally unstable environments in midlatitude events in both hemispheres (Fromm and Servranckx 2003; Fromm et al. 2006).

VolcanicCb were first described in the postclimatic Pinatubo environment by Oswalt et al. (1996), and further examined by Tupper et al. (2005). It was shown that the combined effects of the ongoing ash emissions, secondary explosions, and diurnally warming ash deposits around Pinatubo locally modified the diurnal cycle of thunderstorm activity in the area, bringing forward the daily convective development by a couple of hours and allowing ash transport towards the tropopause. A similar nocturnal effect was tentatively identified at the maritime eruptions of Manam, Papua New Guinea, in 2004/05 (Tupper et al. 2007).

1.5 Motivation for and structure of this study

This study was prompted primarily by the need to further clarify the influence of tropospheric moisture and tropopause height on eruption height and cloud characteristics. In particular, if the large number of volcanoes in the moist tropics are able to produce tall but

ash-poor eruption clouds from relatively weak eruptions, as remote sensing evidence seems to indicate, then a reassessment of our aviation warning system, and particularly the assumption that all eruptions to cruising altitudes produce fine ash at concentrations dangerous to jet engines at those altitudes, may be needed.

In exploring the variation of eruption height in different studies further, we also consider the comments of Sparks et al. (1997, p.119) that, following the modelling of Woods (1993), significant departures from their empirical relationship may be expected in relatively weak eruptions in a moist atmosphere, in conjunction with their summary (p. 109) that ‘...as a simple criterion, eruption columns whose total ascent height exceeds about 12 km are not significantly affected by environmental moisture’. If, in the tropics, a 15 km high cloud can grow over a relatively weak eruption, the height of an eruption cannot be used in itself to determine the eruption intensity. If, however, the effect is more modest than that, as suggested by modelling (Glaze and Baloga 1996; Woods 1993), there is less reason for concern.

We use the ‘ATHAM’ model, described below, to simulate a set of eruptions in idealised volcanic conditions. We vary only the velocity at the vent, to try and gain a sense of whether the model is producing results that look ‘real’ in that context. The eruptions take place in four different atmospheres observed around four different real volcanoes (two tropical, one midlatitude and one polar). We use the same idealised eruptions in these atmospheres, varying only the velocity at the vent. The model also allows us look at the differing composition of the cloud in terms of ash, gas and hydrometeor content under different atmospheric conditions.

We first present the model and its use to date, give a brief discussion of the chosen observed atmospheres and the associated eruption clouds, and then discuss the model results in the context of the above discussion.

2 Numerical methods

2.1 Introduction to the ATHAM model

Studies of meteorological convection show significant differences between 1D modelling results and those from more sophisticated schemes; for example Cohen (2000) found that for environments with a large low-level Convective Available Potential Energy (CAPE), modelled cloud tops could be very different between 1D and 2D models owing to entrainment differences. Similarly, for a more detailed consideration of volcanic cloud development, it is necessary to use a more sophisticated model concept.

ATHAM was developed to explore many aspects of volcanic cloud behaviour (Herzog et al. 1998; Oberhuber et al. 1998). Graf et al. (1999) used the model to examine the effect of phase changes of water and the effect of environment conditions on plume rise.

The aim of ATHAM is to simulate larger spatial and temporal scales than very high-resolution models like those of Valentine and Wohletz (1989) and Dobran and Neri (1993), which can be highly computer intensive (Ongaro et al. 2007). However, ATHAM cannot resolve the processes close to the vent. ATHAM simulates explosive volcanic eruptions for a given forcing as the lower boundary condition, and uses a modular structure to enable ease of modification. The model is three-dimensionally formulated with an implicit time-step scheme; however, to save computer resources, most sensitivity studies have been conducted in either a 2D Cartesian or cylindrical mode; the 2D Cartesian mode to examine cross wind effects, and the cylindrical for simulating entrainment effects (apart from wind-shear

induced entrainment), as in this study. Simulations in cylindrical coordinates reproduce the results from 3D simulations without crosswind.

In its treatment of the so-called active tracers, the effect of ash and hydrometeors on the dynamic is considered, in contrast to usual atmospheric models, where such tracers are passively transported. ATHAM assumes that all particles are small, and are therefore in thermal and dynamic equilibrium with their environment. The thermal equilibrium assumes an instantaneous heat exchange between the components of the system so that particles and gas always have the same temperature. The dynamic equilibrium means zero momentum fluxes between particles and the gas phase. Particles approach their stationary fallout velocity on time scales that are typically in the order of a second or less and are therefore too small to be resolved by the model. All particles move with their terminal velocity relative to the gas phase, allowing for the description of sedimentation.

These assumptions strongly reduce the number of prognostic quantities and allow for the treatment of a multicomponent system with a high number of active tracers. Instead of solving prognostic equations for the momentum and heat of each component only one set of Navier–Stokes equations is required for the volume mean of momentum and heat. Five prognostic equations describe the dynamic behaviour of the gas particle mixture; one for each of the three momentum components, one for the pressure, and one for the temperature. One additional transport equation is taken into account for each tracer. The assumption of small particles is a minor restriction for Plinian eruptions, but more substantial for Strombolian-style eruptions where the magma does not fracture as much.

The turbulence scheme used in ATHAM is described by Herzog et al. (2003). Turbulent exchange is extremely important in a volcanic eruption column because the entrainment of air into a particle-laden plume critically changes the buoyancy of the plume (Sparks et al. 1997). The scheme used in ATHAM is an extension of the Kolmogorov–Prandtl formulation, where the horizontal and vertical components of the turbulent kinetic energy as well as the turbulent length scale are simulated by a set of three coupled prognostic equations. Herzog et al. (2003) compared the results from this scheme with a simplified isotropic scheme, finding that the more realistic approach developed for ATHAM predicted instabilities in the ascending zone, which created a ‘pumping’ motion that resulted in a higher overall plume height. Compared to the simplified scheme the ATHAM scheme leads to a reduction of entrainment and less hydrometeors within the umbrella cloud.

The treatment of condensation processes is very important due to the concurrence of supersaturated water and ash in rising volcanic clouds (Durant et al. 2008; Williams and McNutt 2004). Volcanic clouds are very rich in condensation nuclei due to the number of particles emitted in the eruption cloud. The microphysical processes in the version of ATHAM used here are described by Textor et al. (2006a, b). The hydrometeor microphysics is based on a modal approach and an ash module simulates particle growth and coagulation based on the microphysical interactions between hydrometeors and ash particles. A scavenging module calculates the gas scavenging processes within the plume, considering the effects of the solutes on microphysical processes.

Hydrometeors are described by two size classes (here with mean volume radius 2.5 and 50 μm for small and large particles, respectively), each of which is divided into a liquid and a frozen category. Volcanic particles are analogously divided into four categories. Volcanic particles are assumed to be active condensation nuclei for water and ice formation; hence nucleation is much stronger than in usual meteorological clouds due to the higher number concentration of volcanic ash particles—see Textor et al. (2006a) for a detailed discussion of this parametrisation. Two moments of the distribution, the mass mixing ratio and the number concentration, are calculated as prognostic variables.

The particle size distributions are described with gamma functions. Aggregate mixtures of hydrometeors and volcanic particles can be contained in all four-particle categories. Ash particles sufficiently covered with water or ice are presumed to act in a similar micro-physical manner to pure hydrometeors. Ash and hydrometeors coexisting at a given grid point are assumed to be in mixed aggregates of any composition ranging from wet ash to mud rain given by the sum of the mass mixing ratios of ash and hydrometeors. Hence, this simplified parameterisation excludes the coexistence of dry ash, pure hydrometeors and mixed aggregates at the same grid point.

ATHAM has also been adapted for simulating pyro-Cb (Luderer et al. 2006; Trentmann et al. 2006). These authors have compared ATHAM-simulated pyroclouds above fires with observations in the 3D version of the model. ATHAM reproduced the observed geometrical structures of the Chisholm fire, but simulated (fire) ash concentrations and optical depth were somewhat lower than the measured ones.

It was not possible to closely verify volcanic simulations against observations, generally because of the lack of information about the precise source parameters at the vent. Thus, in the general sense, the cautions of Sparks et al. (1997, p. 115) regarding multiphase numerical models not being verified against observations still apply; nevertheless the model has so far provided valuable insights into processes in strongly convective, particle laden clouds above volcanoes and fires, and as it develops in sophistication more and more realistic simulations are possible. The lack of silicate ash content in pyro-Cb makes them suitable for direct airborne particle sampling, in contrast to volcanic-ash laden clouds, which will damage aircraft (e.g. Casadevall et al. 1996).

2.2 Simulations to date with ATHAM

The setup and the initial conditions used in the previous volcanic ATHAM studies so far, and in this paper, are summarised in Table 1. A wide variety of initial conditions have been used in the effort to make a realistic simulation of a Plinian-style eruption.

An examination of the effect of phase changes of water was done by Herzog et al. (1998). In the tropics, their simulated Plinian eruption column gained three times as much water from the environment through entrainment (mainly from the lower levels) as from the eruption source.

Graf et al. (1999) examined Plinian style eruptions in a number of standard atmospheric profiles (McClatchey et al. 1972). First using 2D Cartesian coordinates, they demonstrated that the model created a realistic flow around the volcano before the eruption, including lee waves and turbulence. They then used the tropical temperature and humidity profile with four different wind profiles to demonstrate a strong reduction in the height of the plume (ash load maximum at 15 km in the no-wind case but 9 km in the standard wind case). They caution, however, that the 2D Cartesian formulation may result in an overestimate of this effect. Using cylindrical coordinates, Graf et al. (1999) showed a significant dependence on (a) tropopause height, (b) stability of the lower troposphere, and (c) water vapour content. They did not vary the eruption strength to explore the effects of these factors in different size Plinian style eruptions.

A fully 3D simulation was presented by Herzog et al. (2003), who used three particle size classes without considering aggregation processes and interaction with cloud microphysics. After 50 min of their eruption only a negligible amount of the smallest ash particles (diameter 20 μm) and 1% of the medium-sized ash particles (400 μm) had been deposited on the ground, but more than 60% of the largest ash particles (8 mm) had already settled out.

Table 1 Initial conditions for volcanic forcing above vent used in published ATHAM papers and here

	Oberhuber et al. (1998)	Herzog et al. (1998)	Graf et al. (1999)	Herzog et al. (2003)	Textor et al. (2003, 2006a, b)	This study
Base diameter (m)	60,150,300	300	300	300	750	750
Vent height (km)	2	2	2.3	~2	0.75	0.75
Grid resolution (boundary, centre) (km)	~5, 0.1	~5, 0.1	~5, 0.1	~5, 0.1	~5, 0.25	~2.5, 0.15
Domain size (x,y,z) (km)	7.5 × 7.5 × 50, 100 × 30 × 50, 200 × 50 × 50	200 × 200 × 50	250 × 250 × 50	250 × 200 × 50	300 × 300 × 50	150 × 150 × 35
Velocity at vent (m s ⁻¹)	250, 205, 131	131	131	250	400	4, 8, 16, 32, 64, 128, 256, 512
Eruption temperature (K)	1200, 1011, 727	727	727	1073	1100	1100
Specific gas concentration of erupted material (kg/kg)	0.03, 0.205, 0.491	0.491	0.491	0.06 (50% H ₂ O)	0.0734 (82% H ₂ O)	0.0734 (82% H ₂ O)
Volume mean density (kg m ⁻³)	5.52, 1.31, 0.80	0.80	0.80	3.143	2.6	2.6
Mass eruption rate (kg s ⁻¹)	3.9 × 10 ⁶ , 4.75 × 10 ⁶ , 7.42 × 10 ⁶	7.42 × 10 ⁶	7.42 × 10 ⁶	5.55 × 10 ⁷	4.5 × 10 ⁸	5 × 10 ⁶ → 6.30 × 10 ⁸

Textor et al. (2003) concentrated on the fate of SO₂, H₂S and HCl, and found that, despite scavenging, more than 25% of the HCl and 80% of the sulphur gases in the modelled strong Plinian eruptions reached the stratosphere. The reason for this unexpected large injection of volcanic gases into the stratosphere was the lack of efficient scavenging agents as the majority of hydrometers were frozen in the cold volcanic cloud. Textor et al. (2006a, b), modelling strong Plinian eruptions with clearly stratospheric umbrella clouds, showed that the presence of hydrometeors, especially liquid ones, in the eruption cloud promotes the aggregation of icy ash particles, strongly increasing their fall velocities. Despite enhanced ice formation resulting from increased humidity in the background atmosphere, the atmospheric humidity had only a small effect on particle aggregation for these strong eruptions (Table 1) apart from a very dry polar case. Particle size distribution, composition and surface properties were found to be very important and not well understood quantities.

2.3 Simulations presented here

These simulations follow Graf et al. (1999) in examining the effect of different atmospheric temperature and moisture structures on the development of eruptions, but using the later refined parameterizations of cloud microphysics and aggregation described above to examine how the height and composition of a range of mainly smaller Plinian size eruption clouds develop in different atmospheres, instead of using a fixed eruption rate.

Vent velocities of $4 \rightarrow 512 \text{ m s}^{-1}$ were used, corresponding to mass eruption rates of $5 \times 10^6 \text{ kg s}^{-1} \rightarrow 6.30 \times 10^8 \text{ kg s}^{-1}$ (Table 1). To investigate the effects of moist processes without cross-wind effects while retaining computational efficiency, the 2D cylindrical mode was used.

Except where otherwise stated, the model setup was that of Textor et al. (2006a) (see Table 1). One set of runs was done using the same grid and generic moist tropical atmosphere (“TROPF”) used by Graf et al. (1999) for comparison purposes, and then the remainder over a smaller and finer domain as shown in Table 1. This gave a horizontal resolution of $\sim 2800 \text{ m}$ at the grid edge, and $\sim 150 \text{ m}$ at the centre, and a vertical resolution of $\sim 500 \text{ m}$ at the top and $\sim 75 \text{ m}$ near the surface.

Comparison between results for the same forcing but different domains showed similar, but more detailed, results for the smaller domain, as expected. An eruption length of 30 min was used—this allowed the maximum plume to be reached (within about the first 10 min) and then a period of steady lateral growth of the plume, capturing all the relevant features and processes in the plume. The model was run for 60 min in total, allowing the cloud to evolve for 30 min after the eruption cessation.

2.4 Characteristics of chosen atmospheric profiles and related eruptions

We emphasise that we are not attempting to properly simulate actual eruptions, but to see what insights the model gives us into how atmospheres into which actual eruptions did occur may have affected the eruption clouds.

The lower parts of the atmospheric profiles used (additional to ‘TROPF’) are described in Table 2 and shown in Fig. 1, and satellite images of the corresponding relevant eruptions are shown in Fig. 2. Most observational soundings have missing data (for example humidity data in the upper troposphere), and balloon ascent to more than 25 km is relatively uncommon. These soundings all reached comfortably into the stratosphere, but in order to create complete profiles suitable for use in ATHAM, some climatologically based

Table 2 Details and indices for atmospheric soundings used in model studies

Station	(a) Kijuchi	(b) Trapani	(c) Momote	(d) Ujung Pandang
Corresponding volcano, summary of atmospheric conditions.	Sheveluch, Kamchatka, Russia. Sub-Arctic spring, dry and stable atmosphere with little wind shear	Etna, Sicily, Italy. Mediterranean summer. Dry, stable	Manam, Papua New Guinea. Equatorial, monsoonal, unstable, moist	Soputan, Sulawesi, Indonesia. Equatorial, unstable, very moist
WMO station number	32389	16429	92044	97180
Observation time/date	00UTC 21 May 2001	06UTC 22 July 2001	00UTC 27 Jan 2005	00UTC 28 December 2005
Station latitude	56.31	37.91	-2.05	-5.05
Station longitude	160.83	12.5	147.42	119.55
Station elevation (m)	29	14	4	14
Convective available potential energy (J/kg)	0	0	2133	509.51
Convective inhibition (J/kg)	0	0	-2.59	-0.13
Temperature (K) of the lifted condensation level	269	285	295	295
Pressure (hPa) of the lifted condensation level	791	892	926	967
Level of free convection (hPa)	N/A	N/A	912	946
Precipitable water (mm) for entire sounding	10	16	55	61

Soundings and indices courtesy University of Wyoming, USA, College of Engineering, Department of Atmospheric Sciences

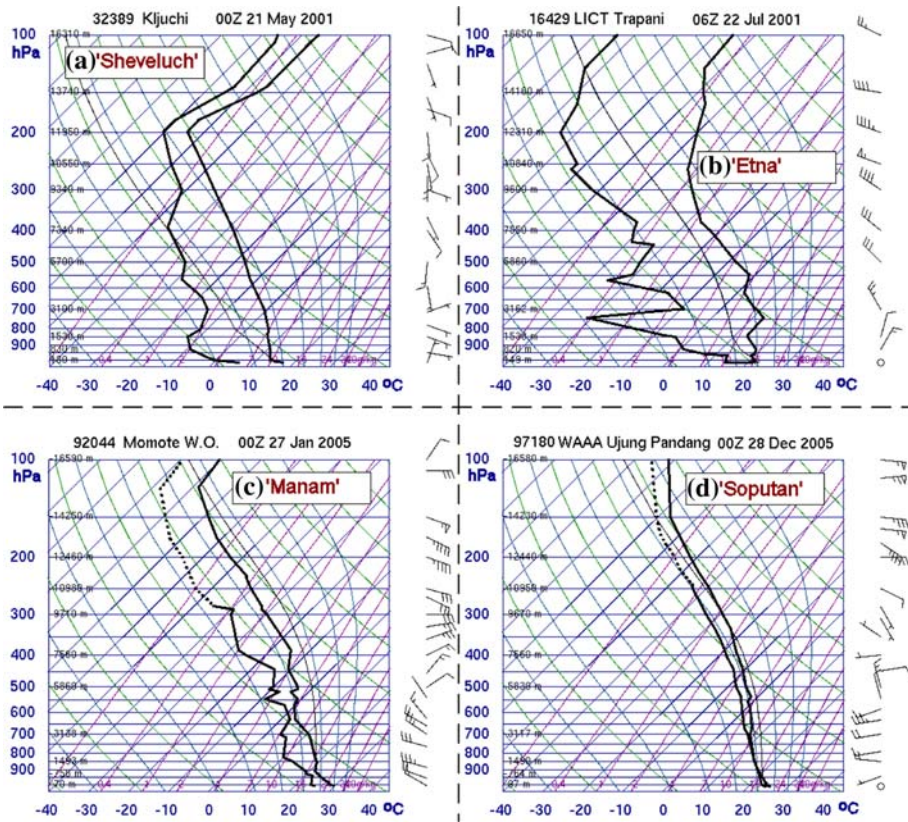


Fig. 1 Observed atmospheric soundings (shown to 100 hPa) as for Table 2. These are shown in conventional meteorological format: in each figure, temperature is plotted to the right of dew-point temperature on the main diagram, and wind observations at corresponding altitudes to the right (the line points to the direction the wind is blowing towards, a half barb indicates five knots, a long barb ten knots, and a flag fifty knots). Data and Skew-T format plotting University of Wyoming, USA, College of Engineering, Department of Atmospheric Sciences. Dotted lines represent extrapolated data (refer text)

missing relative humidity data from the upper troposphere upwards, and temperature data from above the balloon-bursting points in the troposphere were inserted from the appropriate soundings of McClatchey et al. (1972) as used in Graf et al. (1999).

The 21 May 2001 Sheveluch (also spelt ‘Shiveluch’) eruption (Figs. 1a, 2a) was, from the remote sensing point of view, an exceptional event. The cloud, diffusing at different altitudes from the surface to around the lower stratosphere in an almost cloud-free troposphere, had a strong volcanic ash signal and was trackable for approximately 80 h as it first lazily circled Kamchatka within an upper atmospheric high pressure system, and then was captured by westerly winds to head towards Alaska (Tupper et al. 2004). The height of the eruption was unfortunately not well constrained by satellite data and being a night-time eruption the observed eruption height of 20 km from the ground is considered suspect. Although Tupper et al. (2004) allowed for 16 km ± 4 km as an altitude, the most likely height for the cloud was 12–13 km amsl, based on evidence of tropopause temperatures but little stratospheric intrusion.

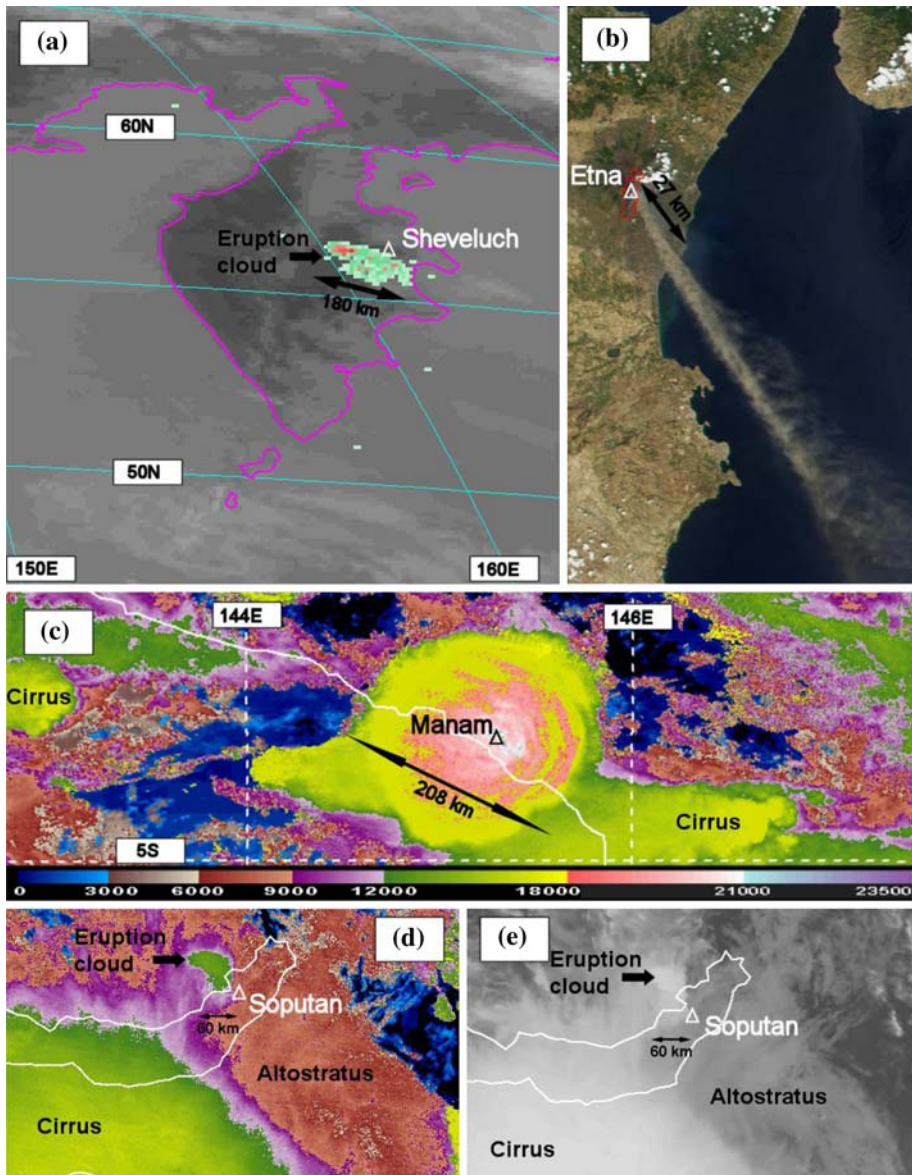


Fig. 2 Eruption clouds and surrounding cloudscape matching above atmospheric profiles: **a** Sheveluch—GMS-5 11 μm image 22 May 2001 0232 UTC, *green/red* indicating ash (see Tupper et al. 2004), **b** Etna—Terra/MODIS True Colour, 22 July 2001 0953 UTC, image and hot spot processing courtesy NASA, **c** Manam—CO₂ slicing heights in metres amsl of Manam umbrella cloud and surrounding clouds using Aqua/MODIS data 27 January 2005 1535 UTC (see Tupper et al. 2007), **d** cloudscape around Soputan eruption, 27 December 2005 0210 UTC (same height scale as **c**), and **e** as for **d** but shown in infrared at 11 μm . The locations of the volcanoes are marked as *triangles*

The vigorous summit and flank eruptions of Mt Etna eruptions from 17 July to 9 August 2001 (sounding ‘b’) were described by Pergola et al. (2004). Examination of ‘CO₂ slicing’ images (Richards 2006), which estimate a cloud height using remote sensing techniques,

for this day suggested a maximum height of the ash plume of about 3.5 km amsl. As can be seen in Fig. 2b, the strong midtropospheric winds (Fig. 1b) and relatively weak eruption appear to have produced a strongly bent over plume, which is clearly visible in a relatively dry atmosphere. Although the actual eruptions themselves were not high in this instance, this situation was chosen as an example case because of the higher (midlatitude) summer tropopause than the Sheveluch example, but still a relatively dry (Mediterranean) atmosphere and a well studied volcano.

The two tropical cases were chosen as being good examples from ‘problematic’ volcanoes in the operational sense. Sounding ‘c’ represents the atmosphere in which the subPlinian eruption of Manam occurred on 27 January 2005; this eruption created a truly impressive stratospheric umbrella cloud but was not detected in real-time for some 14 h due to other monsoonal cloud around and the severing of communications links on the ground (Tupper et al. 2007).

Sounding ‘d’ is representative of the environment that the Indonesian volcano Soputan erupted into on 27 December 2005 (GVN 2006); a very moist and moderately unstable maritime environment with a high water loading (Table 2). The overcast cloudscape is typical for a tropical regime with the very moist atmospheric sounding shown in Fig. 1; the higher-level eruption cloud was unobservable from the ground because of the surrounding cloud, and hence there was a large discrepancy between observed eruption heights from various sources. The eruption had been initially reported at less than 6 km above mean sea level (amsl) on the 27th by an airline pilot, and 1 km above summit height (1,784 m; i.e. <3 km amsl) by ground observers on the 28th. Darwin Volcanic Ash Advisory Centre, on reviewing hourly MTSAT imagery on the 27th, estimated 15 km amsl operationally and then 12.5 km amsl in postanalysis. It would be expected that very few good ground-based observations of eruption clouds produced in these conditions would be extant, and therefore that the observation record may be biased towards clouds produced in drier conditions.

The tropopause in profiles (b–d) is at a similar height (17–19 km) to the soundings used in Graf et al. (1999), but that in profile (a) is significantly lower at ~12 km.

The volcanic forcing in each of these cases is unknown.

3 Results

The presentation of results here focuses on the height and fine ash content of the umbrella cloud region, near the level of neutral buoyancy. Fine ash is most relevant for aviation safety, as it has a long residence time in the atmosphere and can be found at great distances from the volcanic source at cruising altitude. Large ash or aggregates are less dangerous as they are removed from the atmosphere within hours after eruption close to the source.

At the lower mass eruption rates, the differences in the results from moist and dry profiles are very marked; more so than in the previous studies using ATHAM. Figure 3 compares the cloud tops produced by eruptions in the Sheveluch (dry) and Soputan (moist) atmospheres, using the mass eruption rate of $5 \times 10^6 \text{ kg s}^{-1}$. Both runs show umbrella clouds developing in the upper troposphere, near 9 km and 15 km, respectively.

The height of the tropical eruption is much higher due to the additional energy supply from the unstable, moist atmosphere: the umbrella cloud is upper tropospheric or even lower stratospheric and above cruising level (~10 km). The high-latitude umbrella cloud in the dry atmosphere is just below cruising altitude and much less dispersed—it has only about half the diameter relative to the tropical case, and much of the material has stayed at low altitudes due to initial column collapse. However, the amount of fine ash in the small

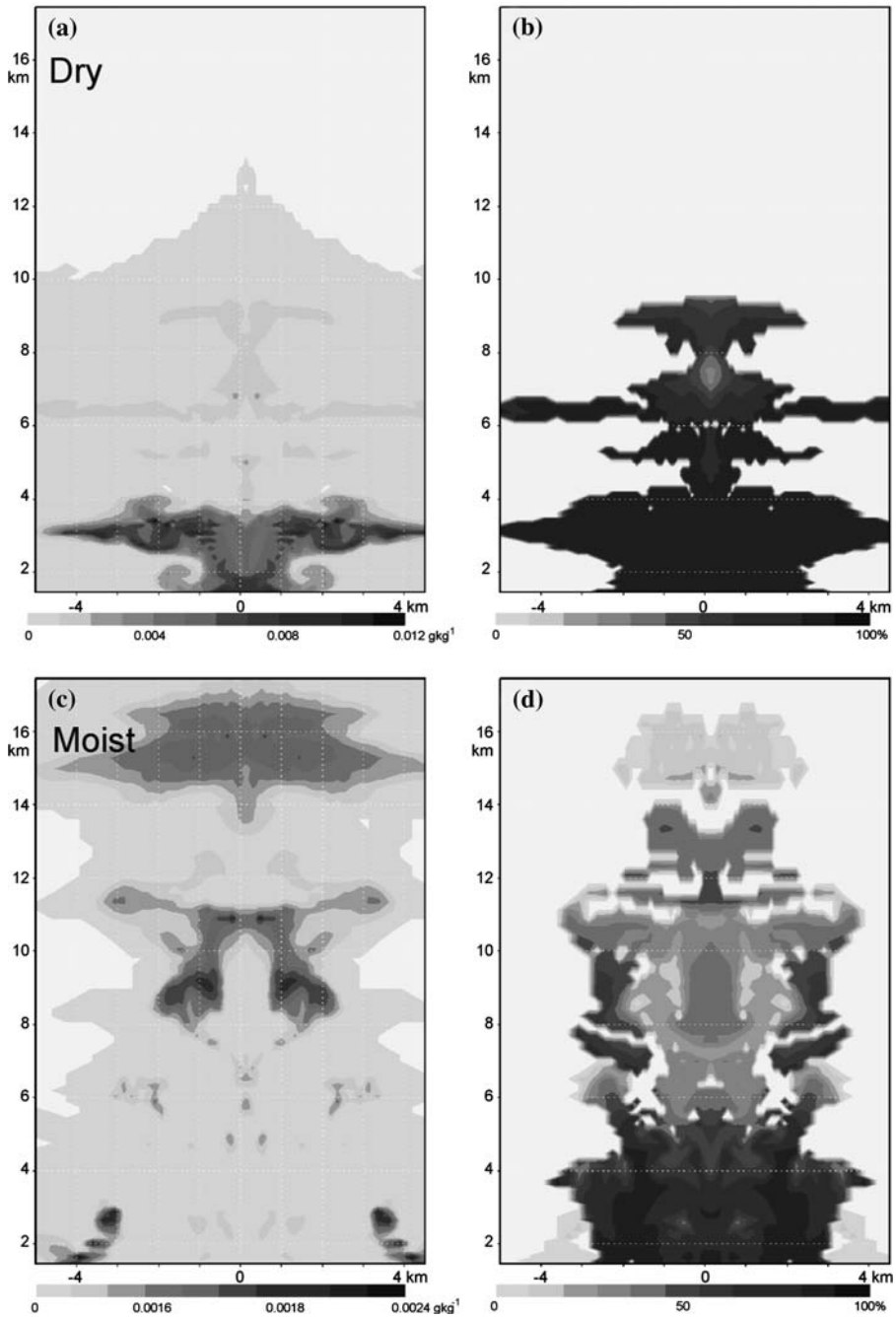


Fig. 3 Total small aggregate classes (ash and water/ice) and fraction of ash for the dry Sheveluch profile (a, b) and moist Soputan profile (c, d), respectively, 30 min after cessation of a modelled eruption with mass eruption rate $5 \times 10^6 \text{ kg s}^{-1}$. The scale in the left hand figures gives minimum and maximum mass mixing ratios in g kg^{-1} tot. mass (note the scale is different in each panel), and the dimensions shown are from 2 to 16 km vertically and the central 9 km horizontally within the cylindrical model domain

aggregates in the tropical cloud is very small compared to the cloud from the eruption in the drier atmosphere, and the amounts of ice in the tropical cloud are very significant.

The differences in eruption cloud dynamics produced in the different profiles are illustrated in Fig. 4, which is a snapshot of the vertical velocities after 20 min of eruption. The peak updraft velocities of 60 m s^{-1} in the ‘Soputan’ case are comparable to the peak convective velocities observed in supercell thunderstorms (Lehmiller et al. 2001) or documented volcanic eruptions (Sparks et al. 1997). The initial velocity used in these particular modelled eruptions was only 4 m s^{-1} , so, as for severe thunderstorms, these velocities have been reached through latent heat release, in addition to the warming at the bottom of the eruption column that is present in both atmospheres.

In both cases, strong convection has developed above the vent, but in the moist tropical case the maximum upward velocities are reached in the upper troposphere as the central column surges towards the tropopause. Although we are cautious to draw analogies that are too close to nonvolcanic clouds (given the higher density of volcanic clouds and their high thermal energy), an upper tropospheric peak in the vertical velocities seems similar to observed deep convection in the monsoon but with an eruption-generated lower tropospheric peak also superimposed, more characteristic of continental surface-heat driven convection (cf Cifelli and Rutledge 1998, Fig. 6a). An alternative analogy might be a

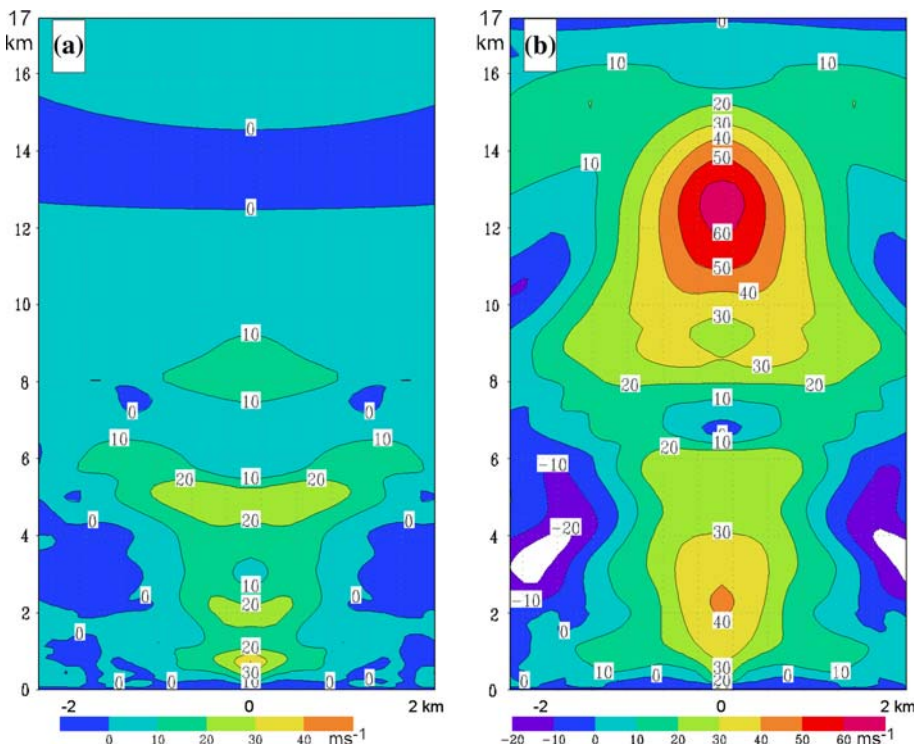


Fig. 4 Vertical velocities during the model eruptions shown in Fig. 3 (20 min into the model run time, and 40 min before the time of Fig. 3), with **a** the Sheveluch profile, and **b** the Soputan profile. Velocities are shown in m s^{-1} (upwards is positive), and the dimensions are shown from 0 to 17 km vertically and 77–80 km horizontally within the cylindrical model domain

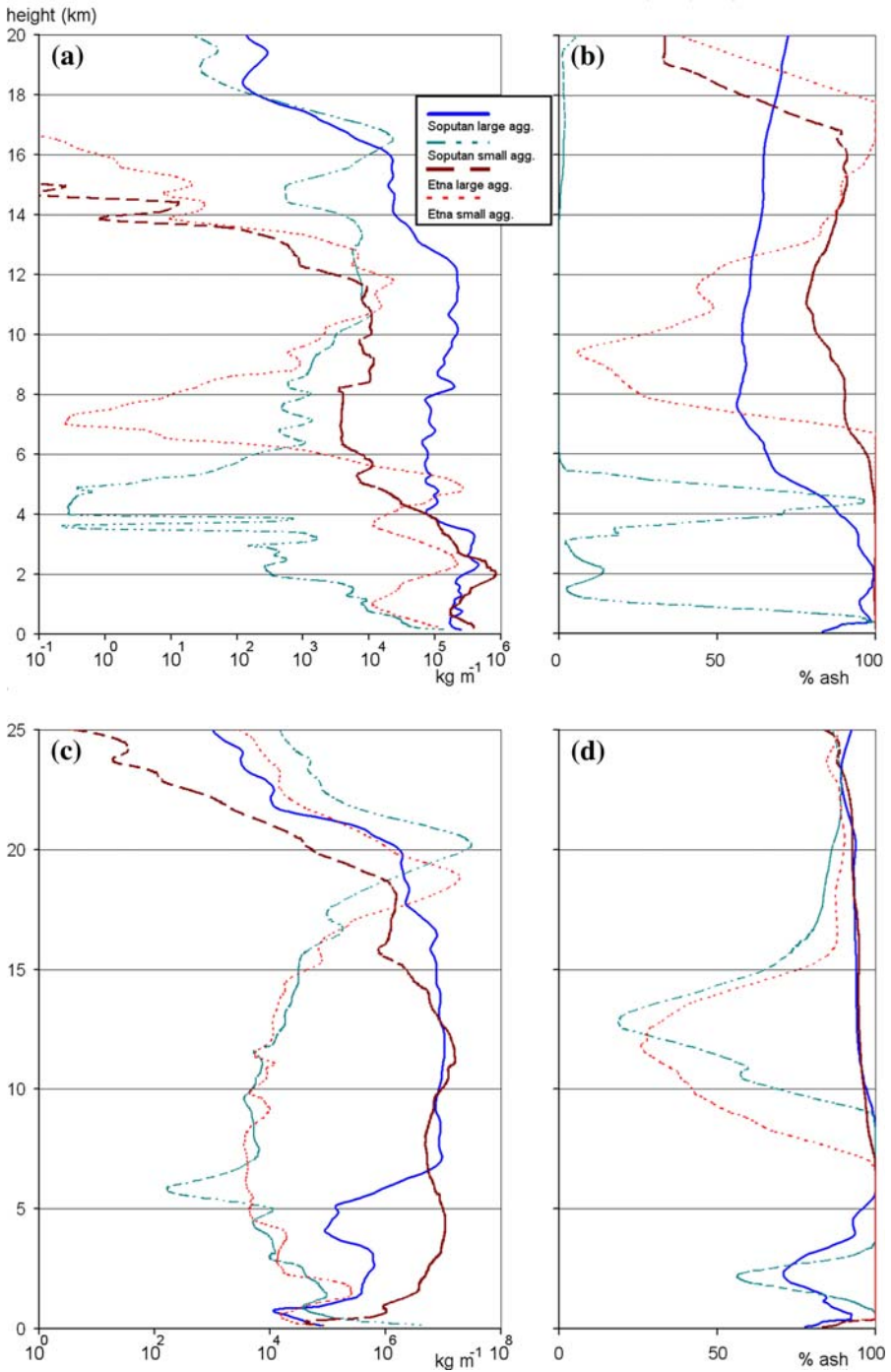


Fig. 5 **a** and **c** Vertical distributions of large (*thick line*) and small (*thin line*) aggregates, and **b** and **d** ash content of those aggregates, for eruption rates of $1 \times 10^7 \text{ kg s}^{-1}$ (*top*) and $3.2 \times 10^8 \text{ kg s}^{-1}$ (*bottom*) from the ‘Sopotan’ (*blue*) and ‘Etna’ (*red*) cases, 30 min after cessation of modelled eruptions

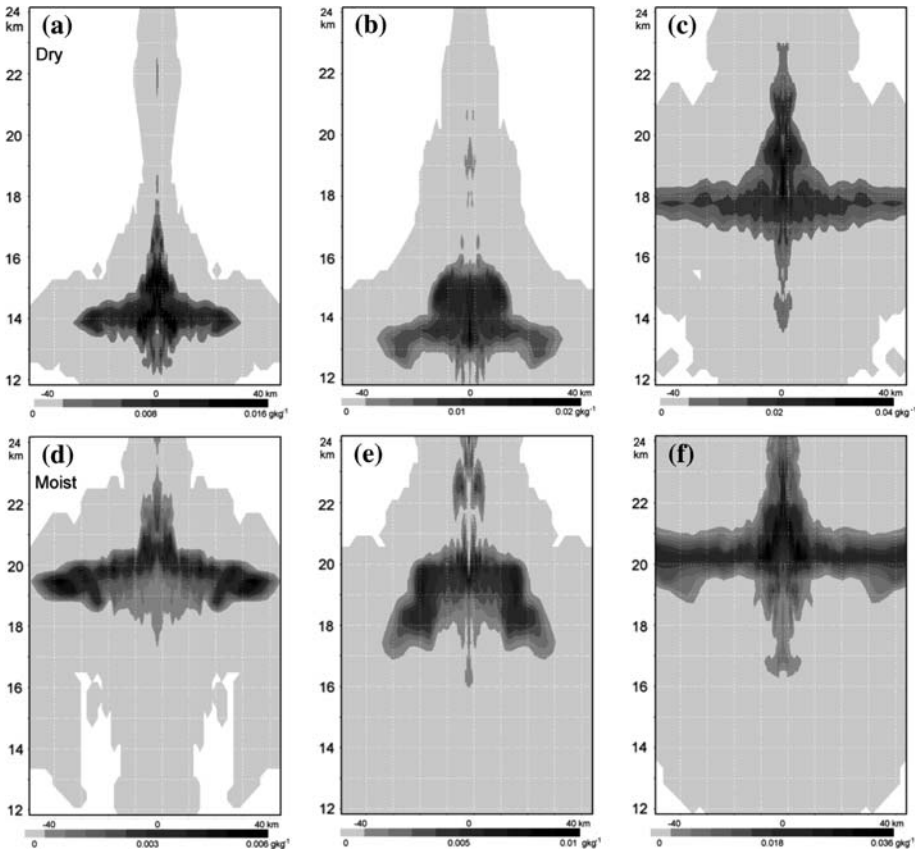


Fig. 6 Total small aggregate classes (ash and water/ice) for the Sheveluch profile (a, b, and c), and for the Soputan profile (d, e, and f), 30 min after cessation of a modelled eruption with mass eruption rates $8 \times 10^7 \text{ kg s}^{-1}$ (a and d), $1.6 \times 10^8 \text{ kg s}^{-1}$ (b and e), and $3.2 \times 10^8 \text{ kg s}^{-1}$ (c and f). The scale gives mass mixing ratios in g kg^{-1} tot. mass (note the scale is different in each panel), and the dimensions are shown from 12 to 24 km vertically and the central 90 km horizontally within the cylindrical model domain. b and e may represent transition states between cross-tropopause and largely stratospheric eruption clouds

tropical maritime squall line, which has a similar vertical velocity profile but with the low level velocity peak driven by gust front uplift (cf Fierro et al. 2008, Fig. 5).

Figure 5 compares ‘Etna’ (dry, but with a higher tropopause than ‘Sheveluch’) and ‘Soputan’ (moist) runs for two stronger eruption rates than for Figs 3, 4. The figure indicates the vertical distributions of small and large aggregates, and the overall fraction of ash at each level in these aggregates.

At the weaker of the two eruption rates (a and b), there is still a large height difference between the umbrella clouds (identifiable by the upper maxima in small aggregate concentrations). The percentage of ash in the small aggregates is very low (near-zero) in the umbrella cloud in the moist case (where high relative humidities in the troposphere help suppress sublimation and evaporation), while over 50% in the dry case. As noted in Textor et al. (2006b), the aggregates tend to dry out below the freezing level, although much less so for the moist atmosphere.

At the stronger eruption rate, the umbrella clouds are nearly at the same height and the aggregates are strongly ash dominant at those altitudes—the effect of atmospheric moisture appears to be very small here. Textor et al. (2006b) discuss the related issues of ice effects on aggregation processes in the cloud.

Figure 6 shows the small aggregates in the umbrella clouds for three successively stronger eruptions in the Sheveluch and Soputan profiles. The transition between partially tropospheric and fully stratospheric umbrella clouds is interesting—in the middle panels, the cloud appears split with a partial collapse back down towards the tropopause. This pattern was common to model runs in all the atmospheric soundings, including the ‘TROPF’ runs in the larger domain, and results in an unexpectedly large step-up in umbrella cloud height between the two highest of the eruption rates shown in this figure, particularly for the drier atmosphere. Further investigation of this feature is left for another study.

Figure 7 illustrates that there is a very weak change in umbrella cloud height with a range of the stronger eruption strengths, but marked differences in cloud composition. Here, we show total SO₂ in the graph in addition to the aggregates, and we also mark the approximate umbrella cloud height for the chosen eruptions. In both atmospheres, the eruptions are forming an umbrella cloud a little above the tropopause, at around 13 km for the Sheveluch (dry) case, and 18 km for the Manam (moist) case. The almost order of magnitude difference in eruption strengths results in a height difference of 1–1.5 km in each case. However, whereas in the Sheveluch case the aggregates in the umbrella cloud are quite dry for both strengths, for Manam there is a definite switch between ice-dominant and ash-dominant smaller aggregates. The relative proportions of total SO₂ also change for the moist case, but not for the dry case.

Figure 8 summarises the height results, including for the initial ‘TROPF’ runs in the larger domain, and compares against the empirical results of Sparks et al. (1997), discussed earlier. Two heights are shown for each model run—the height of the umbrella clouds (solid lines), and an approximate cloud top height (dashed lines). Because of the tendency of the model to sometimes push very small amounts of material up along the central column of the cylinder in a ‘fountain’ effect (apparent in some of the figures), the cloud top height here is defined as being at the altitude where the fine ash concentration is 10⁻⁵ times the concentration at the level of neutral buoyancy.

As expected, there are significant differences in the heights reached by these eruptions, and the dry sub-Arctic profile of Sheveluch generally produces the lowest eruption clouds, with around a 9 km difference in the level of neutral buoyancy between that and the ‘Manam’ profile at the lowest eruption rates, and 10 km or more difference in maximum eruption heights. The decreasing spread of the curves with increasing mass eruption rates indicates the decreasing influence of the atmospheric conditions on the eruption height.

There are some little variations in the general trends—for example, the fact that at the lowest eruption rates the ‘Manam’ clouds are a little higher than the ‘Soputan’ clouds, despite a slightly lower tropopause (~17 km against ~19 km) may reflect the higher Convective Available Potential Energy of that atmosphere (Table 2). The effect of the two lower level inversions in the ‘Etna’ sounding (near 3 km and 5 km amsl) can be seen in the vertical distributions shown in Fig. 5a), and may possibly influence the relative closeness of the Etna and Sheveluch results at lower eruption rates.

The ‘dip’ in umbrella cloud height at higher eruption rates noted for Fig. 6 appears for all profiles in Fig. 8. At the higher eruption rate of $3.2 \times 10^8 \text{ kg s}^{-1}$, the umbrella has become completely stratospheric in all atmospheres.

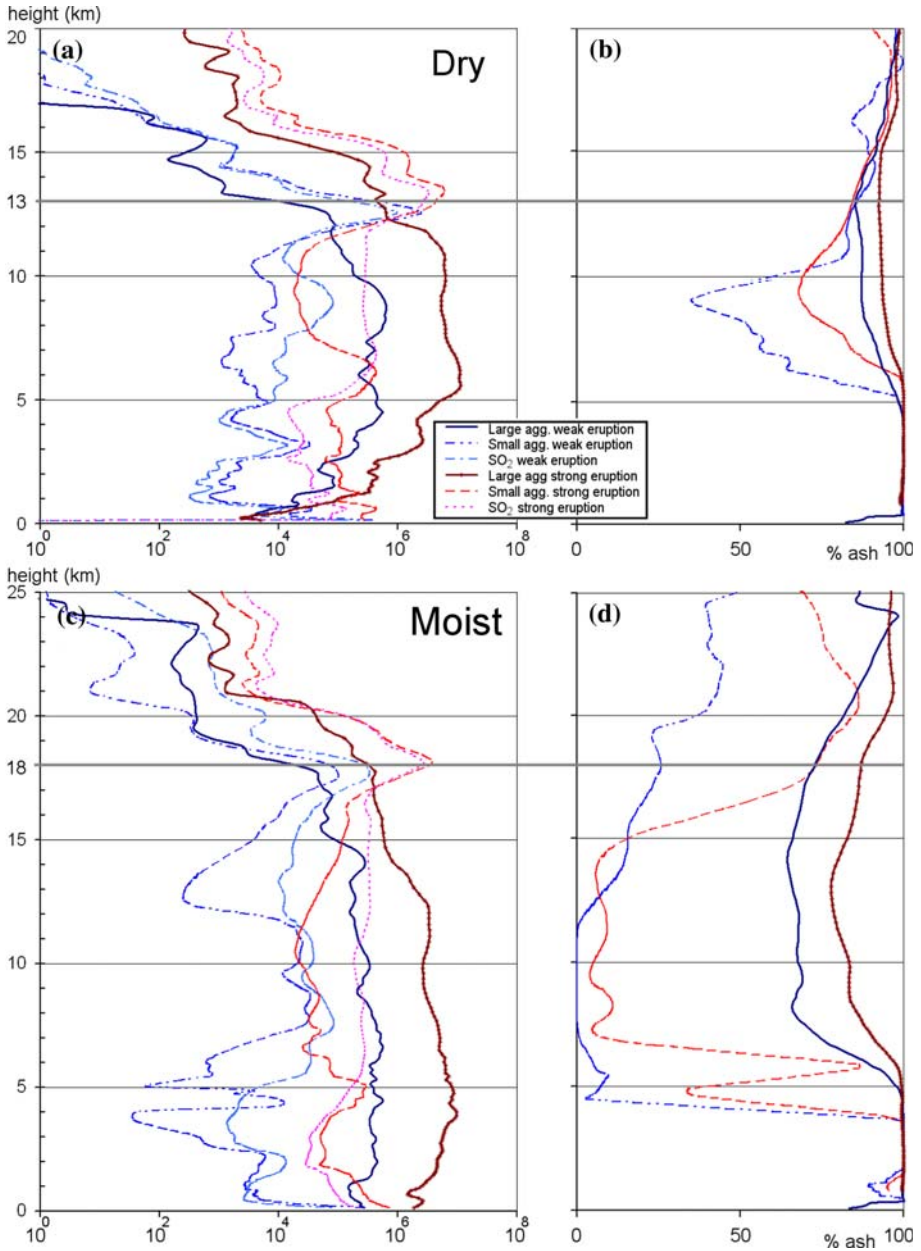


Fig. 7 **a** and **c** SO₂, small and large aggregate vertical distributions for dry ‘Sheveluch’ and moist ‘Manam’ soundings for eruption rates of $2.00 \times 10^7 \text{ kg s}^{-1}$ (‘weak’) and $1.60 \times 10^8 \text{ kg s}^{-1}$ (‘strong’), 30 min after cessation of a modelled eruption. Units for particles are kg m^{-1} and for SO₂ mol m^{-1} . **b** and **d** are the ash fractions of the small and large aggregates for these modelled eruptions. The grey lines in **a** and **c** indicate the approximate mean positions of the umbrella clouds from these eruptions

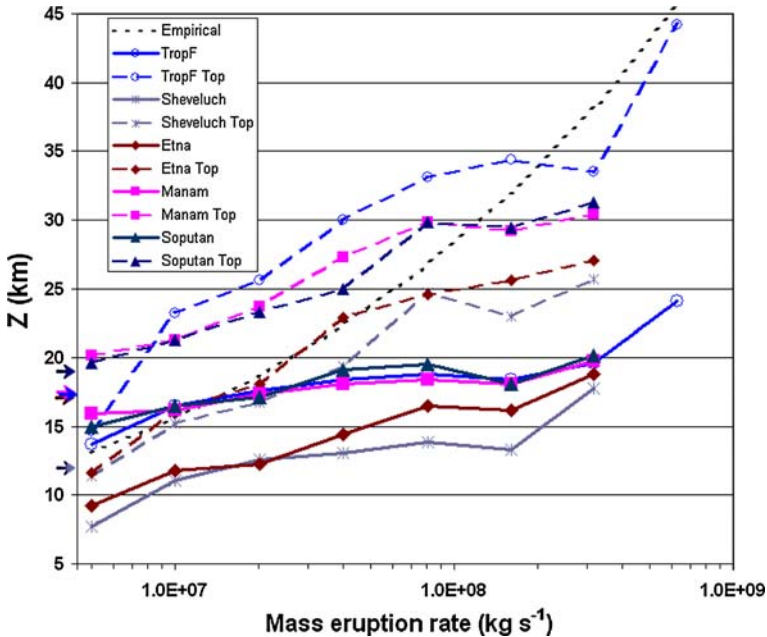


Fig. 8 Neutral buoyancy (umbrella cloud) height, derived using height of maximum mass per height of SO_2 after 1 h of model run time (solid lines), and approximate height of top of cloud (dashed line). Shown for different mass eruption rates in the atmospheres shown in Fig. 1 and for ‘TropF’ from Graf et al. (1999), run on a larger domain to allow the highest eruption rate. The dotted line is from the empirical relation between mass eruption rate and maximum cloud height given in Sparks et al. (1997). The arrows on the y-axis indicate cold-point tropopause heights for the (from bottom) Sheveluch, Etna/TropF/Manam (clustered), and Sopotan atmospheric profiles used

4 Discussion

4.1 Comparison to actual eruption clouds

Although there is no adjustment for volcano characteristics or eruptive style in the simulated forcing, and the cylindrical coordinates used do not allow us to consider wind shear effects, the model gives us insights into the kind of eruption cloud that we might expect into different atmospheres and the relevant cloud processes. Careful application of the model in 3D mode and with realistic initial parameters would hopefully produce a more realistic simulation, but even these 2D results may indicate to an operational meteorologist or volcanologist how a volcanic cloud *might* develop in these different environments given a default eruption.

Comparing the simulations with the real eruptions shown in Fig. 2:

- For Sheveluch, we would expect that a strong eruption might produce a dry, fine-ash rich umbrella cloud near 12–13 km high, and that is what appears to have been observed.
- The Etna eruptions (relatively small, different in style and strongly affected by wind shear) were indeed rich in fine ash and well observable in a dry atmosphere, as we would expect.

- The Soputan eruption of 27 December 2005 (GVN 2006) produced an ice-rich cloud top high in the tropical troposphere (Fig. 2d, e) and like many other volcanic clouds observed in the area, dissipated quickly with no ash signature observed in remote sensing.
- The Manam cloud, which had a well-constrained umbrella cloud topography (Fig. 2c), gave the most interesting results. Figure 8 suggests a neutral buoyancy height of somewhere in the 16–18 km range with an increasing maximum height with eruption strength for the range of simulated eruption strengths, and Fig. 7 shows how the fine ash proportion might be expected to increase with eruption strength. The actual eruption cloud was ice and gas-rich with an observed central overshooting column height of 22–23 km, an umbrella cloud height of around 17–19 km near the edge, and a lidar-observed layer of aerosols left by the eruption at a height of 19 km (Tupper et al. 2007). The Manam heights shown in Fig. 7 are consistent with this, although the level of neutral buoyancy is about 1 km too low when compared to the lidar observations of ash apparently from the umbrella cloud.

4.2 Comparison to previous work on eruption heights

The cloud top height results are very roughly similar to the empirical best-fit curve of Sparks et al. (1997; Fig. 4.11), plotted on Fig. 8. That best-fit curve is fairly approximate: it was based on 28 eruptions, and included maximum height data from direct but presatellite observations of maximum cloud height, isopleth-based umbrella cloud heights, and from a relatively small number of tropical cases. With this in mind, we would expect that the best-fit curve will be somewhere between the height of neutral buoyancy and maximum heights shown, and also that tropical heights will be noticeably underestimated on the best-fit curve due to the combined effects of tropopause height and moisture.

The overall effect of tropopause height shown here appears reasonably consistent with Woods (1993), with the tropopause height appearing to be a strong factor in eruption height between about 5×10^7 and 2×10^8 kg s⁻¹. The main difference is that where the 1D modelling of Woods shows a slight inflection in the variation in ascent height of an eruption as the eruption reaches the tropopause, the modelling here suggests that the tropopause is a more difficult ceiling to break through in terms of the height of neutral buoyancy. To get the umbrella cloud significantly above tropopause height requires an eruption rate of above $\sim 3 \times 10^8$ kg s⁻¹ in these simulations.

There is a notable difference between the modelling here and earlier work in the strength of influence of atmospheric moisture and instability. Graf et al. (1999) had already shown a cloud height variation of 4.5 km (30%) between moist and dry runs using an earlier version of ATHAM and a mass eruption rate of 7.4×10^6 kg s⁻¹, but with a much higher gas fraction (see Table 1). Woods (1993) had suggested a 2–3 km difference in height, and Sparks et al. (1997) showed a 3 km difference in height, for much weaker eruptions than those modelled here, and hardly any moisture-induced variation for eruptions of 5×10^6 kg s⁻¹ and above.

Mastin (2007) used a 1D model to show similar results to Sparks et al. (1997) for weak eruptions, but the plume height difference was maintained for stronger eruptions. Glaze et al. (1997) had ~ 4 km height difference between dry and wet atmospheres for mass fluxes of 6.9×10^7 – 2.7×10^8 kg s⁻¹, and a smaller difference for weaker eruptions. These compare to differences suggested here of up to 9 km in level of neutral buoyancy

height difference or maximum height difference (Fig. 8) for eruption rates of $5 \times 10^6 \text{ kg s}^{-1}$ in different environments.

More important than the absolute height differences, however, is the strong reinforcement of the conceptual model advanced by Woods (1993) that for smaller eruptions there might be an analogy drawn between moisture-driven convective volcanic clouds and pyrocumulus, both of which are highly dependent on the environment for their rise. By using a model that can also simulate pyroCb convection, we are potentially able to take this much further than the earlier modelling. Even with these relatively limited model runs, from Fig. 8 we can think of volcanic plumes in moist and unstable atmospheres as being easily able to develop towards the tropopause and the lower stratosphere, in exactly the manner of a pyroCb generated by a fire.

4.3 Implications for eruption strength estimation

Further to our comments in 1.5, noting the influence of the tropopause (at 12 km in the US Standard Atmosphere but of variable height in real life), and also considering the height range under which nonvolcanic meteorological convection occurs (up to ~ 20 km in the moist tropics), it seems unreasonable to assess either the eruption strength or the effect of environmental moisture on any tropospheric eruption cloud based on height alone. We can simply say that the height of stratospheric eruptions may not be greatly influenced by environmental moisture.

This has consequences for cases where eruption height might be too heavily relied on in determining eruption strength. Newhall and Self (1982) used eruption height as one, but only one, of the diagnostics for their Volcanic Explosivity Index (VEI), and gave a large range of possible heights for each VEI classification. A problem arises for eruptions where only the height is observed, and therefore, it would be important to estimate the tephra volume for cases where eruption height might not be a reliable factor.

4.4 Climate change implications

Climate model simulations and analysis of recent trends show rising of the tropopause, poleward movement of the midlatitude jet stream, and a widening of the tropical belt, observed to be by about $5\text{--}8^\circ$ latitude during 1979–2005 (Seidel and Randel 2007). The widening of the tropical belt is an interesting result as it brings more of the world's volcanoes into tropical atmospheres. The results of this study would suggest that this widening would then result in a rise in average eruption height, but because of the influence of moisture in removing ash, not necessarily an increase in the amount of material reaching the upper troposphere or lower stratosphere.

4.5 Implications for aviation and for remote sensing

These results, including the effect of moisture in removing fine ash from the volcanic cloud, suggest a marked difference in volcanic ash cloud risk for aircraft flying at cruising altitudes ($\sim 10\text{--}12$ km) in different environments. An aircraft flying above a polar winter tropopause might expect to have a reduced chance of encountering an ash cloud, but where one was encountered might expect it to be ash-rich and highly dangerous.

Conversely, an aircraft in the moist tropics would have a relatively high risk of flying into or underneath a volcanic cloud, but if the eruption was relatively weak might only

smell some SO₂ and not notice any fine ash. This does not, however, mean that there is no risk, as most of the more serious volcanic cloud encounters have occurred in the tropics (Casadevall et al. 1996; Johnson and Casadevall 1994), and at this stage even low-grade encounters are thought to pose a significant risk to aviation (Grindle and Burcham 2002; Pieri et al. 2002). The clouds from the Pinatubo eruptions, responsible for the largest number of aviation encounters with ash clouds (Casadevall et al. 1996), were notably ice-rich (Guo et al. 2004a), but as these were strong eruptions, we would expect relatively less ash removal than for the cases shown here (where water/ice acting as a glue for the ash is a very strong factor).

The altitude at which most of the fine ash disperses is also important, but largely not assessed in operations. An awareness of the likely height of neutral buoyancy of a cloud, as well as the height of any inversions would be a critically important part of the hazard reduction strategy of an aircraft, to add to, for example, simulations of traffic density that suggest aviation in the Asia Pacific region will be increasingly vulnerable to volcanic cloud encounters because of the large number of active volcanoes in the region and the increasing growth of air traffic in that region (Prata 2008). Current efforts to improve the dispersion model initialisation for eruptions where limited initial information is available will also be enhanced by greater attention to these issues (Mastin et al. 2009).

As indicated earlier, ice in a volcanic cloud makes it more difficult to identify ash within the cloud. While some techniques exist for trying to determine the relative amounts of ash, ice and SO₂ within a cloud (Guo et al. 2004a, b), the extent of variation in umbrella cloud composition shown here would, if shown to be reflective of real clouds, pose tremendous problems for operational meteorologists and airlines.

An analyst viewing by satellite the tropical eruption clouds for lower eruption rates such as these modelled clouds would most likely see an ice cloud, and if sufficient SO₂ is present, detect some SO₂ using infrared or UV techniques, but would not see any ash, just as was the case for the actual tropical eruptions in Fig. 2. The studied examples of ice-rich clouds show that, where ash signatures are not obvious, clouds can be tracked using SO₂ data (Carn et al. 2003; Prata et al. 2003; Tupper et al. 2004), or through changed particle reflectivity or retrieved particle effective radius (Tupper et al. 2007). Having identified these clouds as ash-poor, it would still be necessary to warn for them while there is no formal safe definition of a concentration of ash (International Civil Aviation Organization 2009).

5 Conclusions

Axisymmetric simulations of volcanic clouds using the numerical model ATHAM and considering ash aggregation suggest that, at weaker eruption strengths, there can be very marked differences between the heights reached by eruption clouds in moist tropical and dry subpolar environments. This is a similar result to the previous Plinian eruption simulations of Graf et al. (1999) without ash aggregation, but the differences appear significantly more marked (~9 km) in height) at lower eruption strengths. The modelling broadly supports the suggestion by Woods (1993) that volcanic clouds in moist atmospheres could have a proportionally lower ash loading and be relatively less of a risk to aviation to eruption clouds at the same heights in dry environments. The model suggests that eruptions into moist atmospheres cause clouds that are higher but significantly poorer in ash than eruptions into dry atmospheres. Because of the relatively higher ice and SO₂

than fine ash loading, the clouds are more difficult to detect as being volcanic using remote sensing ash detection techniques.

These modelling results are consistent with an observed bimodal tendency in cloud heights in the tropics (with a clustering of eruption heights near the tropopause and the ground and a relative lack of midtropospheric maxima) and the number of ice-rich/ash poor high altitude clouds seen in the tropics, including for many eruptions of Soputan and Manam (Tupper et al. 2007; Tupper and Wunderman 2009).

The main implications of these results are that:

- (a) a higher proportion of volcanic clouds will reach aircraft cruising levels in the moist tropics than from drier, more stable, or more poleward environments, but the risk that many of these clouds pose to aviation traffic will be relatively small because of a lower ash content, reinforcing the need to derive an ‘acceptable’ concentration of ash for aircraft, as low-grade encounters in the tropics are likely,
- (b) ash clouds in the moist tropics will be harder to detect and track using remote sensing, as has been reported in various remote sensing studies (e.g. Rose et al. 1995; Tupper et al. 2004),
- (c) eruption intensities cannot be reasonably estimated from eruption cloud heights in the moist tropics,
- (d) eruptions in higher latitudes in dryer atmospheres are less likely to rise to cruising altitudes as they gain their energy mainly from the volcanic source. Clouds at cruising altitudes will however be richer in ash and more dangerous because ash scavenging is less significant, and
- (e) a widening of the tropical atmospheric belt in a changing climate would potentially change the overall climatology of volcanic eruption heights, by bringing more of the world’s volcanoes into tropical atmospheres.

6 Potential for further work

There are some fascinating complexities in the different cloud evolution at various eruption strengths, which deserve to be explored more fully. It would be useful to consider revised parameterisations for the condensation of water on ash particles, for example based on recent examination of ice-sublimation on ash particles for volcanic clouds (Durant et al. 2008). Further, the effects of scavenging and aggregation of small ash particles in the moist environment need additional effort to be simulated adequately. The parametrisation of the effects of the availability of water or ice, the porosity of ash, or electrostatic forces on aggregation efficiency is currently based on theoretical reasoning due to the lack of knowledge of the microphysics of ash and meteorological clouds in volcanic eruption column. Any improvement in these processes might be expected to significantly affect the cloud composition results shown here. Camouflaging dry ash layers in the midtroposphere by overlaying ice in the umbrella region pose another challenge, both to modelling and remote sensing. Further laboratory and field work on volcanic clouds would be extremely useful both for verifying remote sensing and developing realistic modelling.

The effect of small variations in vent height in maritime and continental environments, alternatives to the approach of varying only the initial velocity in order to change the mass eruption rate in these simulations, and the effects of the actual 3D wind fields should be explored, and the small eruption case of ‘volcanicCb’ (Tupper et al. 2005) examined more carefully.

In addition to this further modelling work, well-observed eruptions should have modelled cloud evolution compared to actual and theoretical remote sensing results, in particular using new instruments that provide vertical profiling information such as CALIPSO (Carn et al. 2007). The four eruptions used as the basis for choosing the profiles used in this study were all well observed from space, although the Sheveluch, Manam and Soputan eruptions were not well observed from the ground. Unfortunately, remote areas of the world rarely have major eruptions coincident with good visibility, well equipped volcanological and meteorological observatories and quality polar-orbiting satellite passes, so any opportunity that presents itself along these lines should be seized.

Acknowledgments We thank Larry Mastin and one anonymous reviewer for their thoughtful reviews of an earlier draft of this paper. The first author would like to acknowledge the support of the Australian Bureau of Meteorology, and Monash University in pursuing this work, and particularly that of Geoffrey Garden and Michael Reeder. We would also like to thank Rebecca Patrick for assistance with analysis of the Soputan eruption.

References

- Bursik (2001) Effect of wind on the rise height of volcanic plumes. *Geophys Res Lett* 28(18):3621–3624
- Carn SA, Krueger AJ, Bluth GJS, Schaefer SJ, Krotkov NA, Watson IM, Datta S (2003) Volcanic eruption detection by the Total Ozone Mapping Spectrometer (TOMS) instruments: a 22-year record of sulfur dioxide and ash emissions. In: Oppenheimer C, Pyle DM, Barclay J (eds) *Volcanic degassing*. Geological Society, London, pp 177–202
- Carn SA, Krotkov NA, Yang K, Hoff RM, Prata AJ, Krueger AJ, Loughlin SC, Levelt PF (2007) Extended observations of volcanic SO₂ and sulfate aerosol in the stratosphere. *Atmos Chem Phys Discuss* 7(1):2857–2871
- Casadevall TJ, Delos Reyes PJ, Schneider DJ (1996) The 1991 Pinatubo Eruptions and Their Effects on Aircraft Operations. In: Newhall CG, Punongbayan RS (eds) *Fire and Mud: eruptions and lahars of Mount Pinatubo*. Philippines. Philippines Institute of Volcanology and Seismology & University of Washington Press, Quezon City & Seattle, pp 625–636
- Cifelli R, Rutledge SA (1998) Vertical motion, diabatic heating, and rainfall characteristics in north Australia convective systems. *Quarter J R Meteorol Soc* 124(548):1133–1162
- Cohen C (2000) A quantitative investigation of entrainment and detrainment in numerically simulated cumulonimbus clouds. *J Atmos Sci* 57:1657–1674
- Dobran F, Neri A (1993) Numerical simulation of collapsing volcanic columns. *J Geophys Res* 98: 4231–4259
- Durant AJ, Shaw RA, Rose WI, Mi Y, Ernst GGJ (2008) Ice nucleation and overseeding of ice in volcanic clouds. *J Geophys Res* 113:D09206. doi:[09210.01029/2007JD009064](https://doi.org/10.1029/2007JD009064)
- Ernst GGJ, Davis J, Sparks RSJ (1994) Bifurcation of volcanic plumes in a crosswind. *Bull Volcanol* 56:159–169
- Fierro AO, Leslie LM, Mansell ER, Straka JM (2008) Numerical simulations of the microphysics and electrification of the weakly electrified 9 February 1993 TOGA COARE squall line: comparisons with observations. *Mon Weather Rev* 136(1):364–379
- Fromm M, Servranckx R (2003) Transport of forest fire smoke above the tropopause by supercell convection. *Geophys Res Lett* 30(10):1542
- Fromm M, Tupper A, Rosenfeld D, Servranckx R, McRae R (2006) Violent pyro-convective storm devastates Australia's capital and pollutes the stratosphere. *Geophys Res Lett* 33:L05815. doi:[05810.01029/2005GL025161](https://doi.org/10.1029/2005GL025161)
- Glaze LS, Baloga SM (1996) Sensitivity of buoyant plume heights to ambient atmospheric conditions: implications for volcanic eruption columns. *J Geophys Res* 101(D1):1529–1540
- Glaze LS, Baloga SM, Wilson L (1997) Transport of atmospheric water vapor by volcanic eruption columns. *J Geophys Res* 102(D5):6099–6108
- Graf H, Herzog M, Oberhuber JM, Textor C (1999) Effect of environmental conditions on volcanic plume rise. *J Geophys Res* 104(D20):24309–24320
- Grindle TJ, Burcham FW (2002) Even minor volcanic ash encounters can cause major damage to aircraft. *ICAO J* 57(2):12–14 29

- Guo S, Rose WI, Bluth GJS, Watson IM (2004a) Particles in the great Pinatubo volcanic cloud of June, 1991: the role of ice. *Geochem Geophys Geosys* 5(5):1525. doi:[10.1029/2003GC000655](https://doi.org/10.1029/2003GC000655)
- Guo S, Rose WI, Bluth GJS, Watson IM, Prata AJ (2004b) Re-evaluation of SO₂ release of the climactic June 15, 1991 Pinatubo eruption using TOMS and TOVS satellite data. *Geochem Geophys Geosys* 5(4):Q04001. doi:[10.1029/2003GC000654](https://doi.org/10.1029/2003GC000654)
- GVN (2006) Volcano activity report for soputan. In: Wunderman R, Venzke E, Mayberry G (eds) *Bulletin of the global volcanism network*. Smithsonian Institution, Washington DC, USA
- Halmer MM, Schmincke H-U (2003) The impact of moderate-scale explosive eruptions on stratospheric gas injections. *Bull volcanol* 65(6):433–440
- Herzog M, Graf H-F, Textor C, Oberhuber JM (1998) The effect of phase changes of water on the development of volcanic plumes. *J Volcanol Geoth Res* 87:55–74
- Herzog M, Oberhuber JM, Graf H (2003) A prognostic turbulence scheme for the non-hydrostatic plume model ATHAM. *J Atmos Sci* 60:2783–2796
- Holasek RE, Self S, Woods AW (1996) Satellite observations and interpretation of the 1991 Mount Pinatubo eruption plumes. *J Geophys Res* 101(B12):27635–27665
- International Civil Aviation Organization (2009) *Handbook on the international airways volcano watch (IAVW)*, 2nd edition Doc 9766-AN/968. ICAO <http://www.icao.int/icao/en/anb/met/index.html>, Montreal
- Johnson RW, Casadevall TJ (1994) Aviation safety and volcanic ash clouds in the Indonesia-Australia region. In: *first international symposium on volcanic ash and aviation safety*. Seattle, Washington, USA, pp 191–197
- Lehmiller GS, Bluestein HB, Neiman PJ, Ralph FM, Feltz WF (2001) Wind structure in a supercell thunderstorm as measured by a UHF wind profiler. *Mon Weather Rev* 129(8):1968–1986
- Luderer G, Trentmann J, Winterrath T, Textor C, Herzog M, Graf HF, Andreae MO (2006) Modeling of biomass smoke injection into the lower stratosphere by a large forest fire (Part II): sensitivity studies. *Atmos Chem Phys Discuss* 6:6081–6124
- Mastin LG (2007) A user-friendly one-dimensional model for wet volcanic plumes. *Geochem Geophys Geosys* 8(3):1525. doi:[10.1029/2006GC001455](https://doi.org/10.1029/2006GC001455)
- Mastin LG, Guffanti M, Servranckx R, Webley P, Barsottie S, Dean K, Durant A, Ewert JW, Nerie A, Rose WI, Schneider D, Siebert L, Stunder B, Swanson G, Tupper A, Volentik A, Waythomas CF (2009) A multidisciplinary effort to assign realistic source parameters to models of volcanic ash-cloud transport and dispersion during eruptions. *J Volcano Geotherm Res* in press
- McClatchey RA, Fenn RW, Selby JEA, Volz FE, Garing JS (1972) *Optical properties of the atmosphere* 3rd edition, Air Force Cambridge Research Laboratories, Report AFCRL-72-0497. p 103
- Morton BR, Taylor GI, Turner JS (1956) Gravitational turbulent convection from maintained and instantaneous sources. *Proceedings of the royal society of London A234*(1)
- Newhall CG, Self S (1982) The volcanic explosivity index (VEI): an estimate of explosive magnitude for historical volcanism. *J Geophys Res* 87:1231–1238
- Oberhuber JM, Herzog M, Graf H-F, Schwanke K (1998) Volcanic plume simulation on large scales. *J Volcanol Geoth Res* 87:29–53
- Ongaro TE, Cavazzoni C, Erbacci G, Neri A, Salvetti MV (2007) A parallel multiphase flow code for the 3D simulation of explosive volcanic eruptions. *Parallel Comput* 33(7–8):541–560
- Oppenheimer C (1998) Volcanological applications of meteorological satellites. *Int J Remote Sens* 19:2829–2864
- Oswalt JS, Nichols W, O'Hara JF (1996) Meteorological observations of the 1991 Mount Pinatubo Eruption. In: Newhall CG, Punongbayan RS (eds) *Fire and mud: eruptions and lahars of Mount Pinatubo, Philippines*. Philippines Institute of Volcanology and Seismology & University of Washington Press, Quezon City & Seattle, pp 625–636
- Pergola N, Tramutoli V, Marchese F, Scaffidi I, Lacava T (2004) Improving volcanic ash cloud detection by a robust satellite technique. *Remote Sens Environ* 90:1–22
- Pieri D, Ma C, Simpson JJ, Hufford G, Grindle T, Grover C (2002) Analyses of in situ airborne volcanic ash from the February 2000 eruption of Hekla Volcano, Iceland. *Geophys Res Lett* 29(16):585. doi:[10.1029/2001GL013688](https://doi.org/10.1029/2001GL013688)
- Prata AJ (1989) Infrared radiative transfer calculations for volcanic ash clouds. *Geophys Res Lett* 16:1293–1296
- Prata A (2008) Satellite detection of hazardous volcanic clouds and the risk to global air traffic. *Nat Hazards* 2:235. doi:[10.1007/s11069-11008-19273-z](https://doi.org/10.1007/s11069-11008-19273-z)
- Prata AJ, Bluth GJS, Rose WI, Schneider DJ, Tupper A (2001) Comments on “Failures in detecting volcanic ash from a satellite-based technique”. *Remote Sens Environ* 78:341–346
- Prata AJ, Rose WI, Self S, O'Brien DM (2003) Global, long-term sulphur dioxide measurements from TOVS data: a new tool for studying explosive volcanism and climate. In: *Robock A, Oppenheimer C (eds) Volcanism and Earth's atmosphere*. AGU, pp 75–92

- Richards MS (2006) Volcanic Ash Cloud Heights Using the MODIS CO₂-Slicing Algorithm. In: CIMSS. University of Wisconsin-Madison, Department of Atmospheric and Oceanic Sciences, Madison, p 97
- Robock A (2002) Blowin' in the wind: research priorities for climate effects of volcanic eruptions. *Eos Trans AGU* 83:472
- Rose WI, Delene DJ, Schneider DJ, Bluth GJS, Krueger AJ, Sprod I, McKee C, Davies HL, Ernst GGG (1995) Ice in the 1994 Rabaul eruption cloud: implications for volcano hazard and atmospheric effects. *Nature* 375:477–479
- Sawada Y (1987) Study on analysis of volcanic eruptions based on eruption cloud image data obtained by the geostationary meteorological satellite (GMS). Meteorology Research Institute (Japan), Tokyo, p 335
- Sawada Y (2002) Analysis of eruption cloud with geostationary meteorological satellite imagery (Himawari). *J Geogr (Jpn)* 111(3):374–394
- Seidel DJ, Randel WJ (2007) Recent widening of the tropical belt: evidence from tropopause observations. *J Geophys Res* 112:D20113. doi:[20110.21029/22007JD008861](https://doi.org/10.21029/22007JD008861)
- Settle M (1978) Volcanic eruption clouds and the thermal power output of explosive eruptions. *J Volcanol Geoth Res* 3:309–324
- Simpson JJ, Hufford G, Pieri D, Berg JS (2000) Failures in detecting volcanic ash from a satellite-based technique. *Remote Sens Environ* 72:191–217
- Simpson JJ, Hufford G, Pieri D, Berg JS (2001) Response to comments of failures in detecting volcanic ash from a satellite-based technique. *Remote Sens Environ* 78:347–357
- Sparks RSJ, Bursik MI, Carey SN, Gilbert JE, Glaze L, Sigurdsson H, Woods AW (1997) Volcanic plumes. Chichester, Wiley, p 589
- Textor C, Graf H, Herzog M, Oberhuber JM (2003) Injection of gases into the stratosphere by explosive volcanic eruptions. *J Geophys Res* 108(D19):4606. doi:[4610.1029/2002JD002987](https://doi.org/10.1029/2002JD002987)
- Textor C, Graf H, Herzog M, Oberhuber JM, Rose WI, Ernst GGG (2006a) Volcanic particle aggregation in explosive eruption columns part I: parameterisation of the microphysics of hydrometeors and ash. *J Volcanol Geoth Res* 150:359–377
- Textor C, Graf H, Herzog M, Oberhuber JM, Rose WI, Ernst GGG (2006b) Volcanic particle aggregation in explosive eruption columns part II: numerical experiments. *J Volcanol Geoth Res* 150:378–394
- Trentmann J, Luderer G, Winterrath T, Fromm M, Servranckx R, Textor C, Herzog M, Graf H-F, Andreae MO (2006) Modeling of biomass smoke injection into the lower stratosphere by a large forest fire (part I): reference simulation. *Atmos Chem Phys Discuss* 6:6041–6080
- Tupper A, Wunderman R (2009) Reducing discrepancies in ground and satellite observed eruption cloud heights. *J Volcanol Geotherm Res* (in press)
- Tupper A, Carn S, Davey J, Kamada Y, Potts R, Prata F, Tokuno M (2004) An evaluation of volcanic cloud detection techniques during recent significant eruptions in the western 'Ring of Fire'. *Remote Sens Environ* 91:27–46. doi:[10.1016/j.rse.2004.1002.1004](https://doi.org/10.1016/j.rse.2004.1002.1004)
- Tupper A, Oswalt JS, Rosenfeld D (2005) Satellite and radar analysis of the volcanic-cumulonimbus at Mt Pinatubo, Philippines, 1991. *J Geophys Res* 110(D09204):746. doi:[10.1029/2004JD005499](https://doi.org/10.1029/2004JD005499)
- Tupper A, Itikarai I, Richards MS, Prata F, Carn S, Rosenfeld D (2007) Facing the challenges of the international airways volcano watch: the 2004/05 eruptions of Manam, Papua New Guinea. *Weather Forecast* 22(1):175–191
- Valentine GA, Wohletz KH (1989) Numerical models of Plinian columns and pyroclastic flows. *J Geophys Res* 94:1867–1887
- Williams ER, McNutt SR (2004) Total water contents in volcanic eruption clouds and implications for electrification and lightning. In: 2nd international conference on volcanic ash and aviation safety. Office of the federal coordinator for meteorological services and supporting research, Alexandria, Virginia, USA, pp 67–71
- Wilson LS, Sparks RSJ, Huang TC, Watkins ND (1978) The control of volcanic column heights by eruption energetics and dynamics. *J Geophys Res* 83:1829–1836
- Woods AW (1988) The fluid dynamics and thermodynamics of eruption columns. *Bull Volcanol* 50:169–193
- Woods AW (1993) Moist convection and the injection of volcanic ash into the atmosphere. *J Geophys Res* 98:17627–17636
- Woods AW (1995) The dynamics of explosive volcanic eruptions. *Rev Geophys* 33:495–530
- Woods AW (1998) Observations and models of volcanic eruption columns. In: Gilbert JS, Sparks RSJ (eds) *The physics of explosive volcanic eruptions*. Geol Soc, London, pp 91–114